AIP | Journal of Applied Physics

# Multifunctionalities driven by ferroic domains

J. C. Yang, Y. L. Huang, Q. He, and Y. H. Chu

Citation: Journal of Applied Physics **116**, 066801 (2014); doi: 10.1063/1.4891632
View online: http://dx.doi.org/10.1063/1.4891632
View Table of Contents: http://scitation.aip.org/content/aip/journal/jap/116/6?ver=pdfcov
Published by the AIP Publishing



# Multifunctionalities driven by ferroic domains

J. C. Yang,[1] Y. L. Huang,[1] Q. He,[2] and Y. H. Chu[1,a)]
[1]*Department of Materials Science and Engineering, National Chiao Tung University, Hsinchu 30010, Taiwan*
[2]*Department of Physics, Durham University, Durham DH1 3LE, United Kingdom*

(Received 28 February 2014; accepted 4 April 2014; published online 11 August 2014)

Considerable attention has been paid to ferroic systems in pursuit of advanced applications in past decades. Most recently, the emergence and development of multiferroics, which exhibit the coexistence of different ferroic natures, has offered a new route to create functionalities in the system. In this manuscript, we step from domain engineering to explore a roadmap for discovering intriguing phenomena and multifunctionalities driven by periodic domain patters. As-grown periodic domains, offering exotic order parameters, periodic local perturbations and the capability of tailoring local spin, charge, orbital and lattice degrees of freedom, are introduced as modeling templates for fundamental studies and novel applications. We discuss related significant findings on ferroic domain, nanoscopic domain walls, and conjunct heterostructures based on the well-organized domain patterns, and end with future prospects and challenges in the field. © *2014 AIP Publishing LLC*. [http://dx.doi.org/10.1063/1.4891632]

## INTRODUCTION

Ferroics exhibit spontaneous reversible orders, such as magnetization in ferromagnets, electric polarization in ferroelectrics, and elastic strain in ferroelastics.[1] These materials possess unique hysteretic behaviors that are responsible for different external stimuli, such as magnetic field to ferromagnets, electric field to ferroelectrics, and uniaxial stress to ferroelastics. The ferroic nature enables these materials to be reversibly switched from one state of order parameters to another, which greatly enhanced the controllability and tunability of their physical properties and functionalities. One of the focal features of ferroic materials addressed the spontaneous breaking of the local symmetry. In order to minimize the total free energy in the ferroic materials, domain architectures developed as a result of energy competitions; while within each individual domain, the order parameters present a single ordering state[2–5] (Fig. 1). Ferroic domains in homogeneous materials have captured great attention in applied physics and materials science community over the past decades. For the numerous functional ferroic systems that being explored, multiferroics have recently aroused great scientific interests and thirst, because those materials provide intriguing coexistence and coupling between different order parameters and possess the potential to modulate one through another.[6–10] In this article, using the model system of multiferroic $BiFeO_3$ (BFO), we will capture the progress on advanced domain engineering for creating periodic domain patterns, which serve as fundamental templates to study and discover the intriguing physics and versatile functionalities upon ferroic domains. Furthermore, we will highlight how emergent phenomena driven by the periodic ferroic patterns with conjunct function layers can lead to potential applications of next generation electronics.

Because of the competition and coupling between orders, domain architecture of multiferroics can be more interesting in physics than it is in normal ferroics. It has great potentials to provide special environments to enhance or modulate the ferroic properties or even create new orders or couplings through the coexisting order parameters. Among numerical multiferroics, BFO, the most studied and well-established multiferroics system, has played an important role in renovating this filed after the discovery of its large ferroelectric polarization ($\sim$100 $\mu$C/cm$^2$)[11] with both a high ferroelectric Curie temperature ($\sim$1100 K) and a high antiferromagnetic Neel temperature ($\sim$640 K).[12–14] BFO possesses an *R3c* space group and can be described by $ABO_3$ perovskite pseudocubic structure with spontaneous polarization along the $\langle 111 \rangle$ directions. The presence of the Bi 6*s* lone pair electrons servers as the primary origin of the ferroelectricity of BFO.[15] Two distorted perovskite blocks connected along their pseudocubic $\langle 111 \rangle$ have been used to visualize its crystal structure in which the two adjacent oxygen octahedra rotate in opposite directions and with Fe ions shifted along the same direction on the $\langle 111 \rangle$ axis.[16,17] In bulk, BFO exhibits a G-type antiferromagnetic ordering with Fe spins confined to planes that are perpendicular to the (111)-ferroelectric polarization directions. BFO symmetry allows a small canting of the Fe spins in the material, originated from Dzyaloshinskii–Moriya interaction,[18,19] which generates a weak ferromagnetic moment in the material. After a variety of studies seeking for strong magnetoelectric coupling in BFO,[20–23] Zhao *et al*. revealed that the antiferromagnetic and ferroelectric orders are highly correlated by applying photoemission electron microscopy (PEEM) and piezoresponse force microscopy (PFM) to study the corresponding orders at the same location on the samples.[9] Moreover, they have first unveiled the strong intrinsic coupling between the antiferromagnetism and ferroelectricity by demonstrating the rotation of the antiferromagnetic easy axes when switching the ferroelectric polarization by an external electrical field. It was also one of the very first studies that the researchers could ever directly visualize the entangled order parameters in multiferroics at a nanoscale.

a)E-mail: yhc@nctu.edu.tw

 

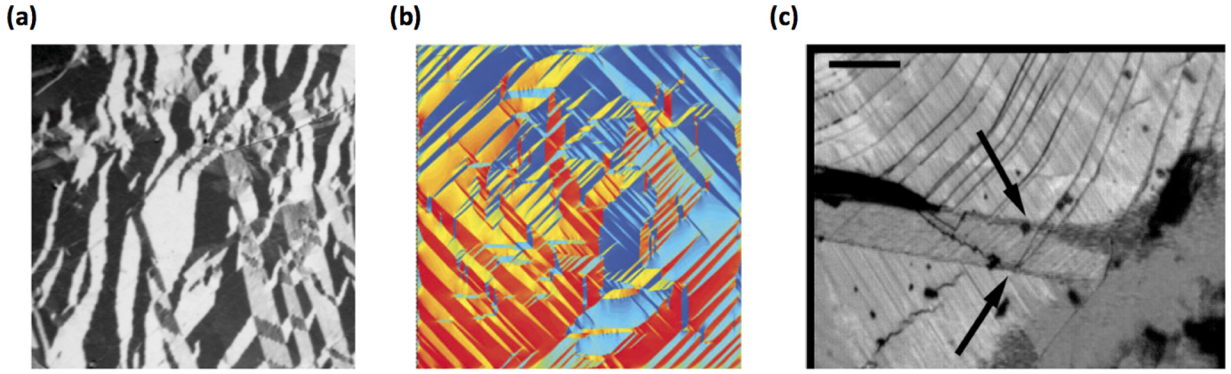


FIG. 1. Examples of ferroic domain structures: (a) ferromagnetic domains in a Co thin film, (b) simulated ferroelectric domain patterns of $BaTiO_3$ nanodots, and (c) ferroelastic twin walls in a $WO_3$ single crystal. Adapted from J. Stohr, *Magnetism: From Fundamentals to Nanoscale Dynamics* (Springer, 2006) (a); Phys. Rev. Lett. **111**, 165702 (2006) (b), and Ref. 68 (c).

In BFO, the arrangement types of adjacent domains are usually described and named by the angle differences between the ferroelectric polarizations in the adjacent domains. Since the ferroelectric polarizations are along the four possible pseudocubic ⟨111⟩ body diagonals in BFO, three different angles can be formed between two adjacent polarizations (71°, 109°, and 180°), suggesting the existence of three types of arrangement between adjacent domains (Figs. 2(a)–2(c)). In our recent study, we have discovered a fourth type of domain arrangement in BFO, the 90° domain relationship, stabilized in an orthorhombic-like BFO phase, which created by exerting anisotropic tensile strain from the substrate.[24] As a consequence of the combination of depolarization field and tensile strain, the ferroelectric polarizations in this phase point in ⟨110⟩ directions, instead of ⟨111⟩ directions (Fig. 2(d)). The transition area between two adjacent domains is a domain wall. In order to maintain the continuity of normal component of electric displacement field across the domain boundaries, different types of domain walls form in their particular planes (except 180° domain wall, which can form in any plane that the ferroelectric polarizations lie). The relationship of domain and corresponding domain wall planes are depicted in Fig. 2. Different types of domain configuration and resulting domain boundaries in ferroic materials can exhibit totally distinct physical properties and functionalities. For example, theoretical studies proposed by Lubk *et al*. by using density functional theory[25] suggested that one could design and modulate the inherent properties of BFO by controlling the formation of its ferroic domains and selection of the domain wall types. However, the complexity and the coexistence of different domain configuration have hindered the exploration of both the fundamental understanding and the potential applications. In the following, we will review the progresses of domain engineering of BFO, leading to the formation of periodic domain patters with long-range ordering. The as-grown periodic BFO domain architecture with controllable domain size serves as a platform to study its intrinsic properties and structure natures, furthermore, a template to offer periodic perturbation to other functional materials that are grown on it.

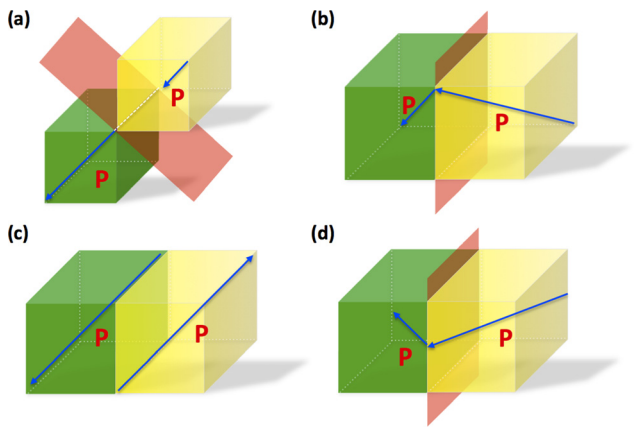


FIG. 2. Schematic of (a) 71°, (b) 109°, (c) 180°, and (d) 90° domain configurations in $BiFeO_3$. The yellow and green bricks respectively represent individual domains with their well-defined polarizations (blue arrows). The red planes represent the domain walls planes in corresponding domain configurations.

## DEVELOP PERIODIC DOMAIN ARCHITECTURE

Preliminary developments of domain engineering were based on the theoretical work proposed by Streiffer *et al*. in 1990s. They have described the generic domain structures of rhombohedrally distorted perovskite ferroelectrics at 1998.[26,27] Domain structures are dominated by the mechanical and charge compatibility of the surroundings.[28,29] The study indicated that the domain patterns of unconstrained rhombohedral distortion along the ⟨111⟩ pseudocubic crystallographic directions would develop with either {100} or {101} boundaries. In rhombohedral BFO, the structural distortion along ⟨111⟩ axes gives four structural variants ($r_1$–$r_4$), as shown in Fig. 3(a). Considering both possible polarization directions on each axis, there are eight polarization variants in the system (polarized up and polarized down) (Fig. 3(a)). In order to form periodic domain patterns at as-grown state with desired types, no more than two polarization variants may be co-existed. To eliminate all other possible polarization variants by tuning the growth process, both elastic and electrostatic boundary conditions have to be taken into account.[30–33] First, orthorhombic substrates providing anisotropic strain are employed to eliminate two structural variants, remaining two structural variants and four possible

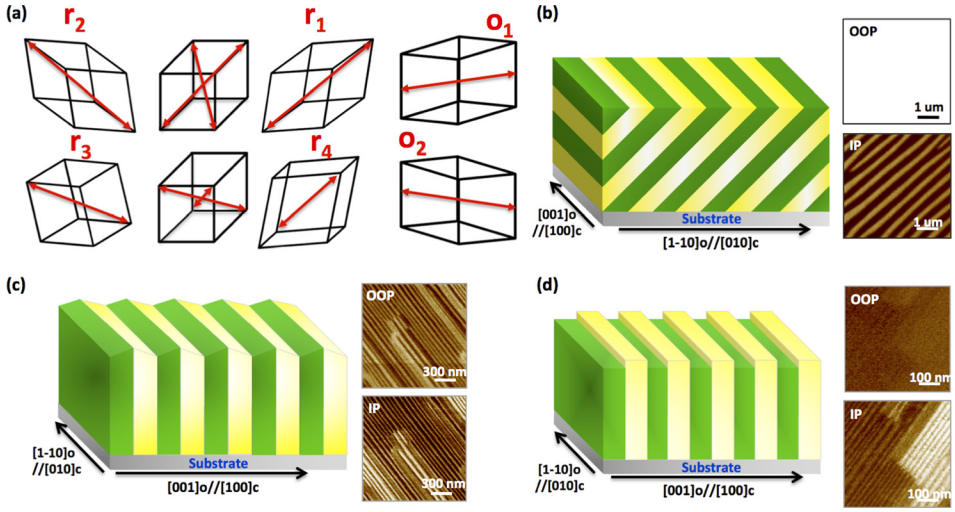


FIG. 3. Domain engineering of periodic patterns in multiferroic $BiFeO_3$. (a) The schematics of structural ($r_1$–$r_4$, $o_1$, $o_2$) and polarization (red arrows) variants. (b) 71°, (c) 109°, and (d) 90° periodic domain patterns shown in schematics (left panels) and corresponding out-of-plane (upper panel) and in-plane (lower panel) PFM images.

polarization directions. The preference of remaining polarization variants is dominated by the electrostatic energy term.[34] Therefore, electro-static boundary condition can be set by the application of bottom electrodes to further eliminate two polarization variants. The presence of free carries at the BFO/substrate interface provided by bottom electrodes forms a built-in electric field, which reduced the activation energy for the nucleation of certain polarized domains.[35,36] This built-in field breaks the equivalence of the remaining polarization variants, leading to a preferential selection of the downward and upward polarization variants (depends on the types of the free carries, electrons or holes). With this method, pure and regular 71° or 109° domain patterns can be successfully grown as perfect arrays in different samples in which the 71° domain walls form on the {101} planes and the 109° domain develop with {100} planes[34] (Figs. 3(b) and 3(c)). The third kind of BFO configuration, 180° domain patterns, was examined by both theoretical and experimental methods in the meanwhile.[37–40] However, it is important to note that the 71° and 109° domain walls are more common in rhombohedral-like BFO films owing to the energy-favorable feature in the distorted structure, while more energy is required to form 180° domain walls and thus it is less identified and seen in periodic domain patterns. A similar approach has been carried on to the domain engineering of orthorhombic BFO phase to form 90° domain pattern. In this case, only the elastic boundary condition is required since there's no out-of-plane polarization component in the orthorhombic phase.[24] The three simplified model systems of periodic BFO domain patterns (71°, 109°, and 90°) are illustrated in Figs. 3(b)–3(d) with the out-of-plane and in-plane PFM images.

To gain further control on the periodic domain patterns, for example the density of domains, is another important step forward to apply those materials in practical electronic devices. Domain size is determined by the energy competition between domain and domain wall and is in delicate balance with the density of domains since forming big domains and domain walls are both energetically costly. In a ferroic film, by minimizing the total energy, including domain, domain wall, and stray-field energy, a square root dependence between domain size and film thickness was proposed by Landau, Lifshitz, and Kittel (LLK) *et al.*,[41,42] known as the famous LLK law

$$w = \sqrt{\frac{\sigma}{U}}d, \tag{1}$$

where $w$ represents the domain width, $\sigma$ is the energy density per unit area of the wall, $U$ is volume energy density of the domain, and $d$ is the film thickness. The relationship can be expressed as $w \propto d^{\gamma}$, where $\gamma$ is the power factor of the relationship. This relationship was originally proposed to apply within the scope of ferromagnetic systems. However, recent studies have shown that the square root dependence of domain width in LLK law generally holds for most ferroics and other periodic domain configurations,[43–45] despite the fact that some exceptional case shows certain deviation to the relationship.[46–50] The domain periodicity v.s. film thickness of different BFO domain configurations as well as classic ferroelectric and ferromagnetic materials are plotted in Fig. 4. Analysis performed on most of the ferroic systems with normal thin film regime (usually in the range of tens nanometers) have yielded exponents closer to the classic value ($\gamma = 0.5$). The deviation from the classic value might

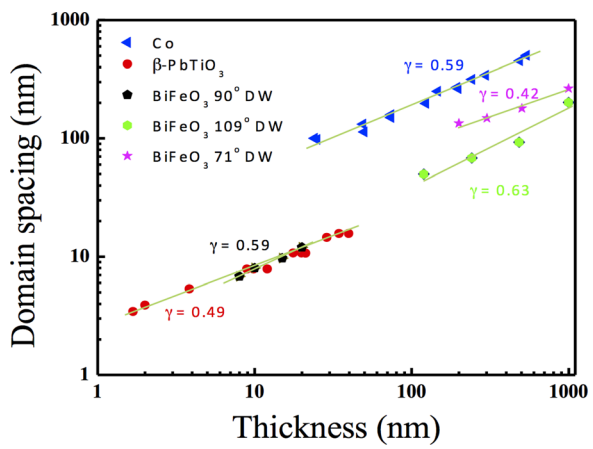


FIG. 4. Periodicity of domain spacing as a function of film thickness in several typical ferroic system. The green lines represent the fitting results of the LLK law and values of $\gamma$ stand for the slopes of the fitting curves. The experiment data of the Co and $PbTiO_3$ are adapted and re-drawn from Ref. 50.

offer certain practical consideration, such as the roughness of the domain walls, screen effect, defect, and the interaction between the adjacent domains.[51,52] Using the quantitative estimation of the LLK relationship enables us to gain further control of the ferroic materials in domain engineering.

## ROLES OF PERIODIC PATTERNS: STRUCTURAL NATURE

The well-controlled periodic domain patterns can be exploited to study the structural nature and competing energy terms of the ferroelectric domains. Nelson *et al.* have revealed the existence of unusual triangular-shaped vortex nanodomains in the 109° domain patterns. They revealed that the vortex closure exhibits properties tremendously different from the surrounding domains, such as a mixed Ising-Néel character of the domain boundaries and a drastic increase of in-plane polarization[53] (Fig. 5(a)). For 109° domain patterns, the system lowers its cost in electrostatic energy by forming alternating out-of-plane polarization to reach the zero net surface charge. The local depolarization field at the termination of 109° domain boundaries nears the uncompensated interface and surface significantly affects the stability of the local polarization and domain structure. As a result, triangle domains consist of a mirrored pair of inclined 180° domain walls forming a vortex domain structure with polarization rotating about the intersection of two 180° and 109° domain boundaries were observed in which the bound charge of the vortex structure forms to suppress the depolarizing field, and thus lower the total electrostatic energy (Figs. 5(b) and 5(c)). In the 109° domain pattern with vortex closure, the 180° and 109° domain walls in the vortices show gradual rotations of the polarization vector exhibiting a mixed Ising-Néel character. Owing to the fact that the polarization normal to 109 °BFO domain boundaries is regarded as the driving force for the charge-screening mechanism resulting to their conductivity.[54] The authors have also suggested that the increased in-plane polarization might be an important factor altering the local electronic properties. Reversed domains can be developed from an existing favorably oriented site within the vortex domains, instead of from a nucleation site and, therefore, the understanding of the stability of the vortex domain via periodic domain patterns is important since they alter switching dynamics while reversing the domains. Further study investigated by Qi *et al.* revealed the structural nature of 109° domain patterns with coexistence of the vortex structure and charged domain boundaries, which affects the physical properties of the entire thin film.[55] The charged boundaries with bound charges can serve as the pinning centers during polarization switching, and can be used to understand the imprint and fatigue issues in data storage applications.[56] The information gained from the presence of the charged domain boundaries in periodic domain patterns also offers further understanding of modulating the domain size and type within ferroelectrics.

## ROLES OF PERIODIC PATTERNS: DOMAIN WALLS

Adjacent domains meet forms a domain wall, serving as a natural interface and providing the spatial transition area between adjacent ferroic domains. In contrary to the interfaces between layers in heterostructures formed by the conjunction of different materials, domain walls are formed within the same material and thus are recognized as homo-interfaces.[57] Intrinsic nanoscopic features of domain walls are of particular interest, because the specific strain states and polar boundary conditions can lead to dramatic changes from their bulk properties and give rise to new functionalities that are absent in their parent materials.[58,59] The special transitional ordering within the domain walls may modify the

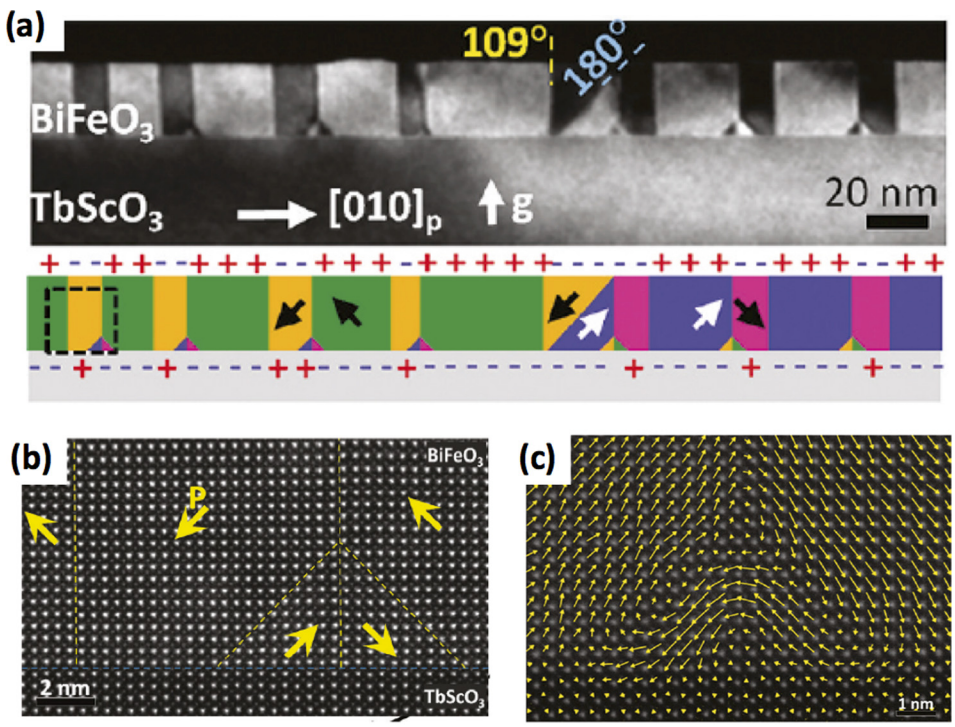


FIG. 5. Observation of spontaneous vortex nanodomains in $BiFeO_3$. (a) Striped 109° domain pattern shown in cross sectional TEM (upper panel). The corresponding domain structures and the distribution of surface/interface charges are schemed in the lower panel. (b) Z-contrast image of two 109° domain walls. The yellow arrows depict the polarizations recognized by the displacement of the Fe cations, where the dashed lined indicate the positions of the domain walls. (c) Displacement plot of the Fe cations of an enlarged 109° domain pattern, where a vortex closure is formed by the presence of a pair of 180° triangle nanodomain. Adapted from Ref. 53.

spin and orbital interactions, electron band structures, and energy degeneracy, etc., resulting in distinct local electronic and magnetic structures from its adjacent domains (bulk properties). In order to study the intrinsic properties and advanced functionalities of the nanoscopic domain walls, the periodic domain pattern can provide a modeling template to unveil the striking physical properties and advanced functionalities.

Significant attention of domain walls has arisen since interesting physics and novel functionalities were discovered. In the earlier work, researchers have addressed that the existence of domain walls can help to stabilize and enhance the material properties.[60–63] Later on, researchers have started to study the domain walls not only as triggering media in the materials, but also as active functional components with their own distinctive properties. In this period, special attention has been driven to the ferroic systems that have structural, electronic, or magnetic properties extremely sensitive to the local physical environments. In theory work, Janovec and co-workers have predicted that the domain walls in multiferroic could be ferromagnetic even though the adjacent domains themselves are antiferromagnetic or paramagnetic[64,65] in 1997. Taking the similar idea further, Daraktchiev and Catalan *et al*. have proposed a Landau-type thermodynamic model to study the magnetism of the domain walls in certain multiferroics.[66,67] Meanwhile, several experimental investigations and classic discoveries have also addressed the importance of the domain walls in ferroic systems since 1990 s. Through the chemically deoxygenated process using a gas transport reaction with Na vapour, Aird and coworkers have unveiled the superconductivity at the domain walls in $WO_3$ in which the preferential doping along the ferroelastic domain walls was ascribed to induce the 2D superconductivity[68] (Fig. 6(a)). This discovery was an important work to the reproducible creation of sheet superconductivity at domain walls in non-superconducting materials. In the study of Ca-doped lead orthophosphate, Bartels *et al*. have revealed that the significant conductivity differences between the ferroelastic domains and domain walls can be controlled via the doping concentration.[69] Meier *et al*. have also demonstrated the electrical conductance of ferroelectric domain wall in hexagonal $ErMnO_3$ described by a continuous function of the domain wall orientation.[70] The consequence of carrier accumulation and band-structure changes in $ErMnO_3$ resulted in the variation of the conductance at the domain walls (Fig. 6(b)). The intriguing insulating-paraelectric states at domain walls in $YMnO_3$ has been investigated by Choi *et al*.[71] They have examined that the ferroelectric state is more conducting than the paraelectric state in this material. In a recent study, Sluka *et al*. have explored the presence of the free-electron gas at charged domain walls in ferroelectric $BaTiO_3$.[72] Their work has revealed that 90° head-to-head charged domain walls in tetragonal and ferroelectric $BaTiO_3$ possessing metallic behavior with enhanced conductivity $\sim 10^9$ times higher than the conductivity of bulk $BaTiO_3$ (Fig. 6(c)). The conducting charged walls only exist in tetragonal phase $BaTiO_3$; as a result, the charged and conducting domain walls would be annihilated at the structural transition points. Furthermore, the conduction mode of this system also shows a change from metallic-type to thermal activated conduction with temperature variation. This study has also implied that the two-dimensional electron gas could be electrically displaced, erased, and recreated in a real device, which paved the pathway toward to new class of nanoelectronics. Moreover, mesoscopic metal-insulator transition has been studied at ferroelastic domain walls of $VO_2$ by Tselev *et al*.[73] The strain-induced metal-insulator phase transition around the ferroelastic domain walls nucleated at temperatures several degrees below the bulk transition, leading to the formation of the conducting paths in the material (Fig. 6(d)).

In addition to the ferroelectric and ferroelastic systems in ferroic family, the potential applications of the domain walls in ferromagnetic systems have gained increasing attention worldwide. More recently, the concept of "domain wall logic" has been proposed for developing a new magnetic logic architecture, which generates very little heat during data switching process and does not require any transistors. The domain walls in ferromagnetic materials are mobile interfaces and can be propagated and controlled by the application of external magnetic fields. The detailed domain wall logic architecture, which based on planar magnetic wires less than a micrometer width, has been constructed and reviewed by Allwood *et al*.[74] Within the scope of the magnetoelectronic applications, Thomas *et al*. have made possible the motion of the domain walls with much less currents (five times smaller than originally required) by using a short train of current pulses and corresponding resonantly amplified oscillation in the domain walls.[75] Extending the concept one step further, Parkin and co-workers have made considerable contributions and efforts in memory devices based on motion of the magnetic domain walls, the so-called "racetrack memory."[76,77] The racetrack memory is composed by a ferromagnetic nanowire in which the domain walls are formed at the boundaries between magnetic domains that are magnetized in opposite directions. The main advantage of such memory is that the spatial positioning of the domain walls can be controlled by the current pulse with high precision.[77] In such case, domain walls act as data bits and are moved to and fro along the racetrack memory in which the data bits can be designed to be read and write with various methods[78–80] (Fig. 6(e)). The hint behind those charming discoveries and application indicates domain walls in ferroic brands a key role in the pursuit of the innately three-dimensional microelectronic devices.

The discovery and understanding of mysteries within ferroic domain walls can be significantly facilitated and thoroughly comprehended via periodic domain patterns. As described in previous paragraphs, the domain architectures can be well controlled by applying proper boundary conditions, resulting in periodic two-variant domain configurations. Through the ordered fashion of BFO domains, transport measurements as a function of temperature along the 109° domain walls was performed to reveal the conduction mechanism[81] (Fig. 7(b)). The conduction behaviors of 109° domain wall can be characterized by two distinct regimes. At low temperature ($T < 200$ K), the transport mechanism can be described as a variable range hopping

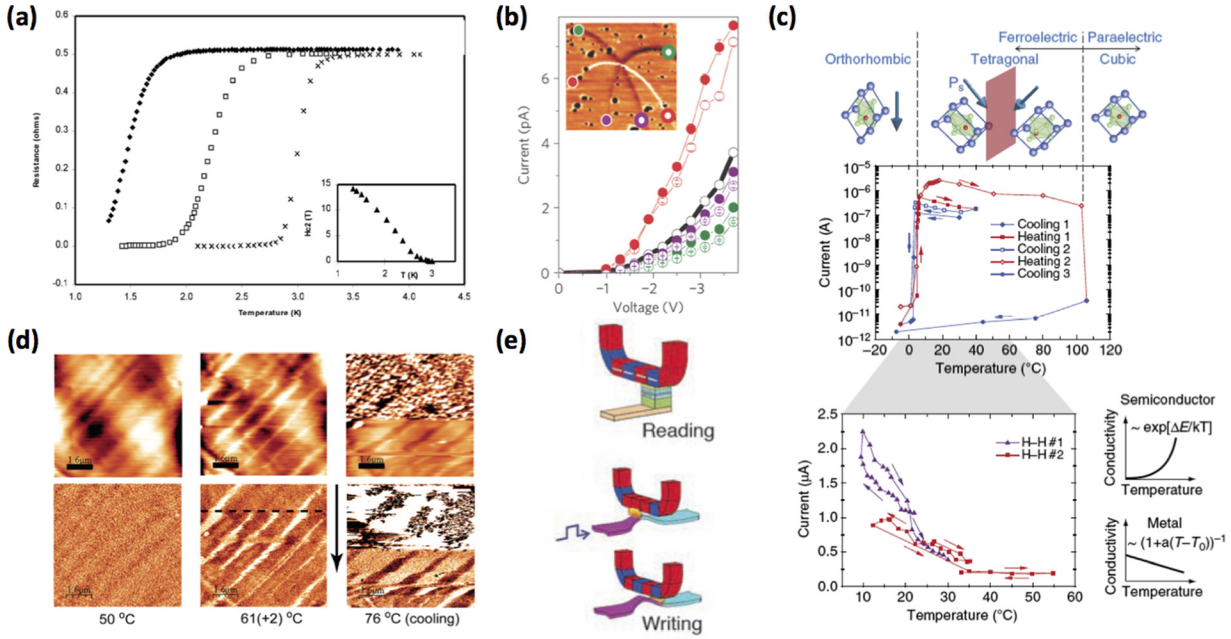


FIG. 6. New properties and functionalities at ferroic domain walls. (a) Two-dimensional superconductivity in $WO_3$. The insets indicate the temperature dependence of $H_{c2}$. (b) The anisotropic electrical conductance at $ErMnO_3$ ferroelastic domain walls. The inset indicates the measured positions of the conducting domain walls. (c) Quasi two-dimensional electron gas at charged ferroelectric domain walls in $BaTiO_3$. (d) Metal-insulator transition at ferroelastic domain walls in $VO_2$. Direct evidence of semiconductor-to-metal transition provided by AFM topography (upper row) and scanning microwave microscopy images (lower raw). (e) The racetrack memory of ferromagnetic nanowires. Adapted from Refs. 68, 70, 72, 73, and 76 for (a)–(e), respectively.

(VRH) process, whereas the transport behaves in a thermally activated mode (with activation energy $\sim 0.25$ eV) above 200 K. Furthermore, a remarkable negative magnetoresistance (MR) were observed when both transport currents and magnetic field were parallel to the domain walls, as shown by Fig. 7(c). A MR value $\sim -60\%$ was observed at a magnetic field up to 7 T. It is more striking that very little MR is measured when the magnetic fields were applied perpendicular to the transport currents (both in-plane and out-of-plane). A general theme of the magnetic field dependence of the core spin orientation and the related influence on electron transport was proposed to conceptually explain the microscopic origins of the MR behavior. The significance of the large magnetoresistance discovered in 109° domain patterns via mass transport offers a promising route toward to the novel functionalities driven by magnetic and electrical stimuli.

The novel multifunctionalities and the small size feature of ferroic domain walls are the focal keys that are thirsted for new generation nanoelectronics. The nanoscopic feature

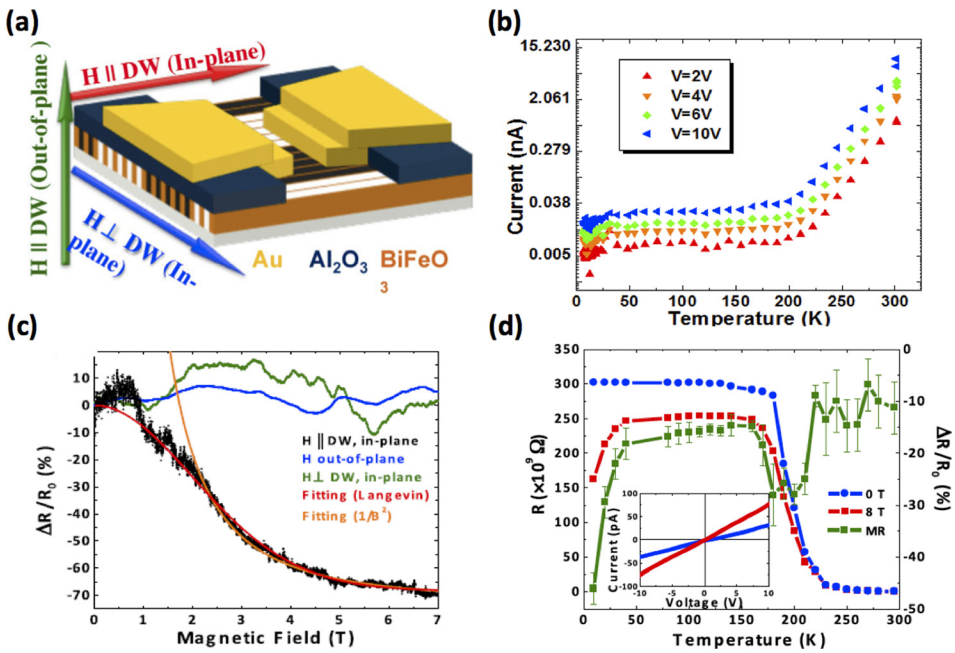


FIG. 7. Transport and magnetotransport studies at 109° $BiFeO_3$ domain walls. (a) Device configuration for transport measurements. The green, red, and blue arrows show the directions of the applied magnetic field. (b) Temperature-dependent current-voltage curves, where a clear transition at can be identified at ~200 K. (c) The magnetoresistance with respect to applied magnetic fields in different directions. (d) Resistance-temperature plots at two different external magnetic fields (0 T and 8 T), where the green curve represents the corresponding magnetoresistance. The linear I-V curves in the inset identify good ohmic contact condition of the device through the whole measurement process. Adapted from Ref. 81.

of the domain wall in multiferroic BFO in which ~2 nm width of domain wall is experimentally revealed by transmission electron microscopy and cross sectional scanning tunneling microscopy.[54,82] Researchers worldwide have done many significant works for demonstrating the potential of these conducting homointerfaces for promising device applications.[83,84] A prototype of the domain wall electronic was demonstrated by Seidel *et al*. for building up the concept of domain wall logic and memory devices taking the advantage of the conduction of nano-sized domain walls.[54] The study has shown that the total current increase proportionally to the total number of the written domain wails, which is consistent to mass transport result.[81] In addition, the increment/decrement behavior of measured resistance exhibits a completely reversible manner during the writing/erasing procedure, promising a possible rewritable, multi-configuration application of multiferroic domain walls driven by the conductive channels at nanoscale.

Far beyond the functional domain walls discovered with the assistance of the periodic domain patters, such a template can also be used to develop new functionalities driven by ferroic domains themselves. Photovoltaic effect in BFO periodic 71° domain patterns has been discovered and revealed by Yang *et al*.[85] For conventional solid-state photovoltaics, the electron-hole pairs are generated by light absorption in a semiconductor, followed by the separation in electrical field in depletion region. The semiconductor band gap is usually the maximum photovoltage of the device could reach. In the study, Yang *et al*. reported a fundamentally new mechanism for photovoltaic charge separation, which produces open circuit photovoltages that are significantly higher than conventional solid-state photovoltaics and the bandgap of the parent material. The photovoltaic device was made on BFO sample with periodic 71° domain walls in which a large photo induced open-circuit voltage can be measured when the electrode for electronic transport are perpendicular to the periodic patterns (Fig. 8(a)). The separation of the carriers takes the advantage of the nanoscale steps of the electrostatic potential that naturally exist in the ferroelectric domain walls of BFO. Such a device makes use of the built-in potential steps of the periodic domain pattern, which arise from the component of the polarization perpendicular to the walls. Once the excited electron-hole pairs are generated, they are then separated and drift to opposite sides of the walls, which builds up the excess of charges. Since the observed photovoltaic effect is driven by build-in electrostatic potential of the ferroelectric domains, the phenomenon is highly related to the types of domain patterns. In a later study, the photovoltaic effect was also observed in periodic 109° domain patterns by Guo *et al*.[86] Despite the fact that the open circuit voltage measured in 109° domain patterns is much smaller than that of 71° domain patterns, the study has implied an important role played by domain walls and corresponding domain configurations. Further experiments conducted by Bhatnagar *et al*. have elucidated that the bulk photovoltaic effect is at the origin of the observed photovoltaic effect in BFO via temperature-dependent measurements with respect to both 71° and 109° domain patterns[87] (Figs. 8(b) and 8(c)). All of those results suggested that the increasing of the number of domain walls enclosed in the circuit would lead to a higher open circuit voltage. The ferroelectric nature enables the photovoltaic effects driven by the periodic domain patterns to be electrically reversed or turned off, which adds new degree of controls in applications in optoelectronic devices.

## FUNCTIONALITIES DRIVEN BY CONJUNCT HETERO-STRUCTURES

Employing periodic domain patterns as templates or platforms, more intriguing properties and novel functionalities may be discovered in the conjunct materials grown on such domain patterns. The tangled ferroic order parameters in multiferroics provide a talented nature to imprint the unique environment and periodic perturbation to heterostructures via various coupling mechanisms. Of particular interests in recent studies, the combinations of multiferroic and ferromagnets have recently been used to achieve the electric-field control of local ferromagnetism in the pursuit for low-energy consumption memory and logic devices.[10,88–91] Previous studies have demonstrated an electrical control of the magnetic anisotropy in piezoelectric-ferromagnet heterostructures.[92,93] Heterostructures composing of $Cr_2O_3$, $YMnO_3$, and $LuMnO_3$ has been used to demonstrate the electrical control of exchange bias.[94–97] However, the restricted experimental conditions (low temperature or assistance of external magnetic field) make the system hard for pursuing practical applications. To extend the goal further, researches have proposed to use room temperature multiferroic BFO for resolving aforementioned challenges. In the study of Heron *et al*., via depositing the ferromagnetic $Co_{0.9}Fe_{0.1}$ (CoFe) layer onto periodic 71° domain patterns, the reversible and deterministic reversal of the magnetization of CoFe at room temperature have been successfully demonstrated.[88] In such heterostructure, a one-to-one correlation of the ferroelectric and ferromagnetic domains was unveiled by a combination of PFM and PEEM. As shown in Fig. 9(a), the ferromagnetic domains of CoFe mimic the periodic ferroelectric domains of BFO in which the magnetizations are discovered to be collinear with the in-plane projection of the corresponding ferroelectric polarizations. The projection of canted moment of BFO can be deduced via the regular manner and well-controlled structural variants of 71° domain patterns, and was unveiled to be parallel to the projection of both the net in-plane ferroelectric polarization and ferromagnetic magnetization. The canted moment of BFO was suggested to play a key role resulting in the magnetic coupling of the heterostructure. The consequential effect of 180° rotation of net in-plane polarization on the canted moment in the $BiFeO_3$ layer and magnetic moment in CoFe were deduced by using anisotropic magnetoresistance (AMR) measurements (Fig. 9(b)). The AMR experiments evidenced that the magnetization of CoFe rotates with the net in-plane polarization of ferroelectric BFO via magnetic exchange coupling, leading to a non-volatile magnetization switching by electrical field. The result took great advantage of the intrinsic coupling of the ferroelectricity and antiferromagnetism in multiferroic BFO in which the 180° phase change of

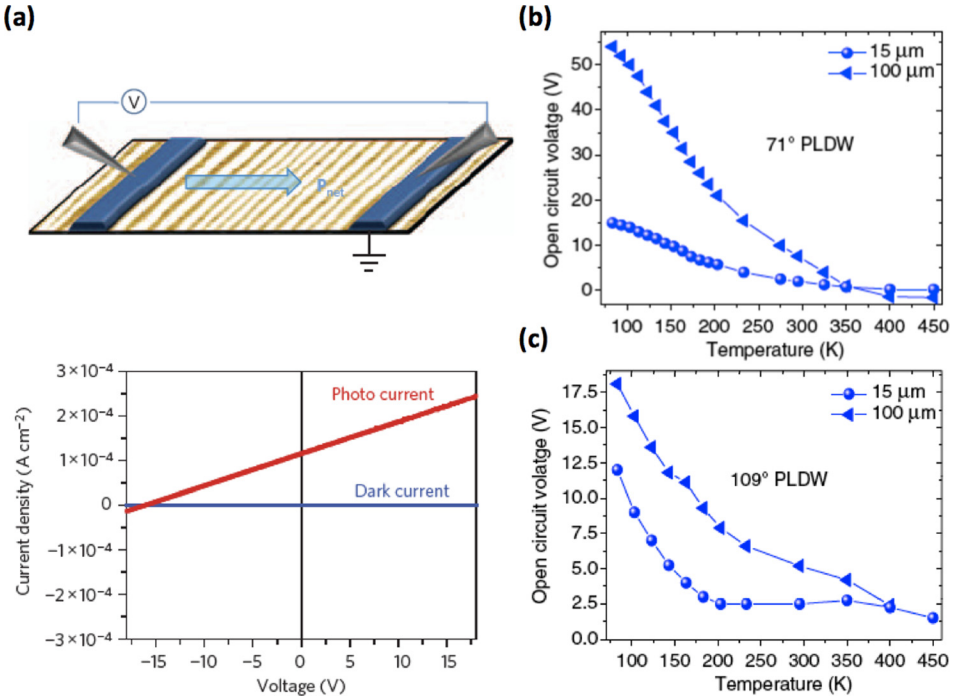


FIG. 8. Photovoltaic studies of periodic domain patterns. (a) Photovoltaic devices made of $BiFeO_3$ 71° domain patterns (upper panel). The lower panel shows the measured light and dark current-voltage curves. The temperature dependence of open-circuit voltages for 71° (b) and 109° (c) domain patterns with electrodes running parallel to domain walls. Adapted from Ref. 85 (a) and Ref. 87 (b) and (c).

polarization of BFO gives rise to the change in the sign of the magnetic torque experienced by magnetization of CoFe ferromagnets (Fig. 9(c)). This finding offered a new insight for the field of spintronics, allowing electric field driven magnetic reversal on practical devices.

In addition to magnetic coupling found in aforementioned polycrystalline heterostructures, periodic domain patterns of ferroic system can offer additional electric, magnetic, and structural perturbation to the heterostructures, which can be precisely controlled via tuning domain periodicity. For example, $La_{0.7}Sr_{0.3}MnO_3$/BFO (LSMO/BFO) heterostructures (Fig. 10(a)) have been used to study the structural coupling between epitaxial ferroic heterostructures.[90,91] A uniaxial magnetic anisotropy was found in LSMO thin film epitaxially grown on periodic 71° BFO domain pattern (Figs. 10(b) and 10(c)). Through the combination of magnetic force microscopy and PFM, the authors revealed the magnetic domains of LSMO mimicking the periodic ferroelectric patterns of BFO (Figs. 10(d) and 10(e)). The magnetic easy axis of LSMO and polarization of BFO

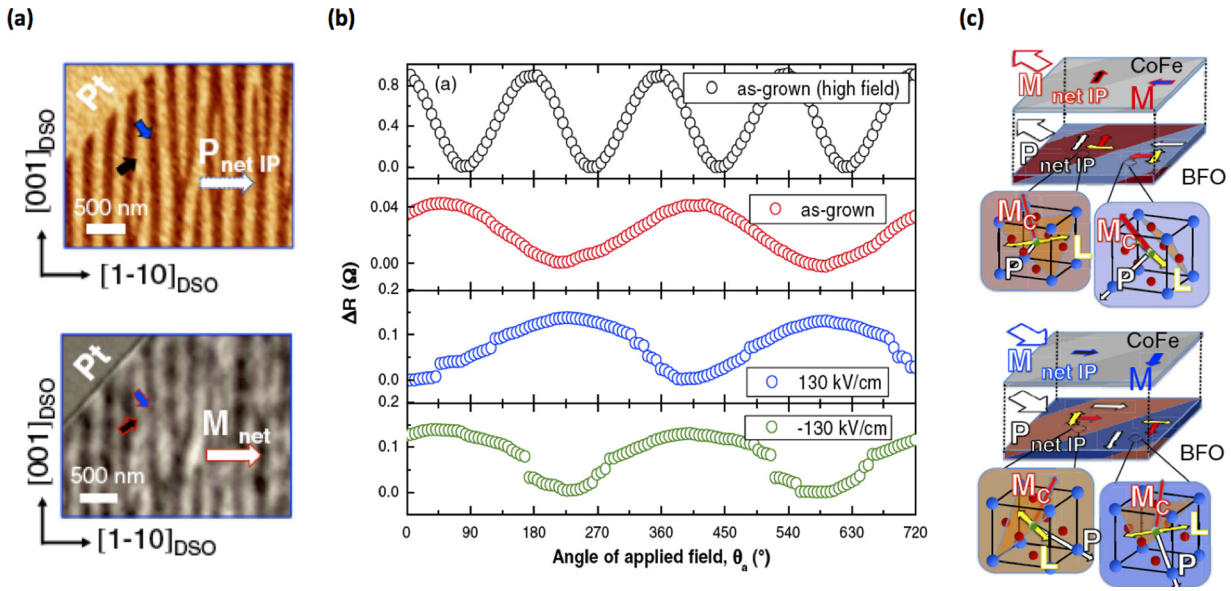


FIG. 9. An electric-field-driven magnetization reversal in a ferromagnet/multiferroic heterostructure. (a) One-to-one correlation of the ferroelectric domains in BFO (PFM image in the upper panel) and ferromagnetic domains in CoFe (PEEM image in the lower panel). (b) AMR studies of the magnetization reversal process. High magnetic field decouples the magnetic coupling between the ferromagnetic and ferroelectric layers (black curve), while low field AMR responses unveil the effect of the magnetic coupling between CoFe and BFO. Positive and a followed negative electric pulse flip the magnetization of CoFe by 180° (blue curve) from original state (red curve) then back to the as-grown state (green curve). (c) The schematics showing the deduced correlation of the net magnetization of CoFe and in-plane polarization of BFO before (upper) and after (lower) electric switching process. Adapted from Ref. 88.

show parallel coupling, which is similar to the finding in CoFe/BFO system (Fig. 10(f)). However, the observed stripe domains in LSMO persist even with the insertion of $SrTiO_3$ interlayer suggested that the coupling between the two ferroic materials is elastic rather than magnetic in nature. The one to one correlation and the uniaxial magnetic anisotropy in such epitaxial system was examined to be aroused from the lattice coupling across the heterostructure. The striking pattern transfer between ferroelectric and ferromagnetic layers could also be seen in CoFe/$BaTiO_3$ system.[98] Those results indicate the ferroic patterns themselves can also be treated as a natural template to imprint various perturbations to the conjunct layer. The utilization of periodic multiferroic patterns can offer more than that. Taking material with coexisting electrical and magnetic orders as an example, such system might be designed to offer periodic fluctuation of local charge, uncompensated spin, polarization bound charge, and even electrical potential steps, for modulating a variety of physical properties, such as superconductivity, colossal magnetoresistance, metal-insulator transition, or even photonic responses. Also, those finding sheds the light on additional degrees of freedom to trigger new functionalities (Fig. 10).

## FUTURE PERSPECTIVE

In the last section of this review, we will discuss future perspectives and challenges for the functional domain patterns. When it comes to the intrinsic properties of ferroic domain patterns, the ordered ferrioc patterns have paved an elegant route toward to progressive scientific investigation and fascinating applications, while the new possibilities to enhanced properties and to advanced functionality modulation can also be achieved by composing heterostructures of periodic ferroic domains, active layers, or even existing functional devices. The general scheme for discovering and exploiting multifunctional systems via periodic ferroic domains are illustrated in Fig. 11. Development of domain engineering act as a starting point to manipulate the couplings between charge, spin, orbital, and lattice degrees of freedom of as-grown domains and domain walls. Boundary conditions in ferroic systems, such as elastic and electrostatic boundary conditions, are the keys to control the domain structures and thus the corresponding domain walls. The progresses of the synthetic approaches such as molecular beam epitaxy and pulsed laser deposition have offered great tools to impose epitaxial constrains to the ferroic systems, which always brought addition surprise to the complex interaction within the nanoscopic feature.[99–101] Also, the advanced scanning probe techniques with nano-scale resolution have served as main keys fueling these developments.[102–106] Another front of the research is how to design or acquire a ferroic material which itself a multifunctional component. One possible solution is to utilize so via the coexistence of order parameters in multiferroics. This is why we take the multiferroic system as a good example for exploring new opportunities within ferroic systems. The development of the domain engineering in BFO thin films, which is one the most

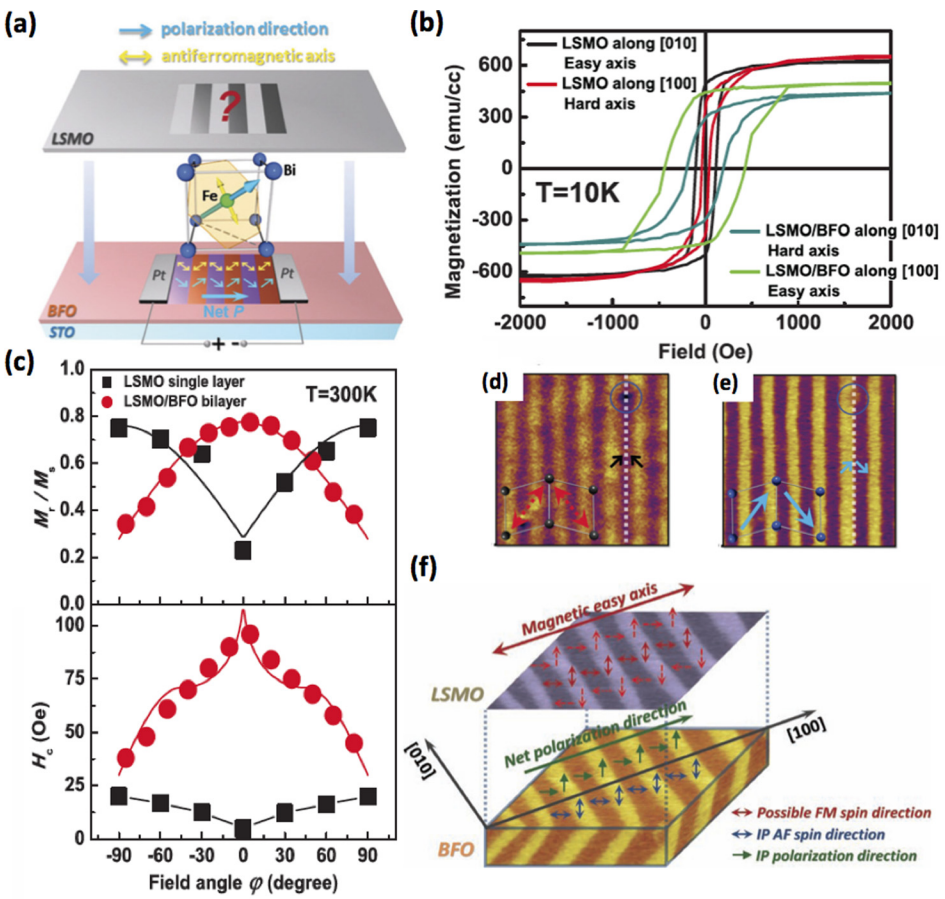


FIG. 10. Uniaxial magnetic anisotropy formed in ferromagnet/multiferroic heterostructure. (a) A schematic of the epitaxial $La_{0.7}Sr_{0.3}MnO_3/BiFeO_3$ heterostructure. (b) In-plane M-H curves along the [010] and [100] directions for a $La_{0.7}Sr_{0.3}MnO_3$ single layer and a $La_{0.7}Sr_{0.3}MnO_3/BiFeO_3$ heterostructure. (c) The corresponding in-plane angular dependence of $M_r/M_s$ and $H_c$ for both samples. (d) The ferromagnetic domains in LSMO imaged by magnetic force microscopy. Red arrows indicate the magnetic easy axes in different domains. (e) Corresponding ferroelectric domains in BFO imaged by PFM. Blue arrows show ferroelectric polarization in corresponding domains. (f) Schematic of the relationships between the in-plane polarizations, antiferromagnetic axis, and coupled magnetic easy axis of the heterostructure. Adapted from Refs. 90 and 91.

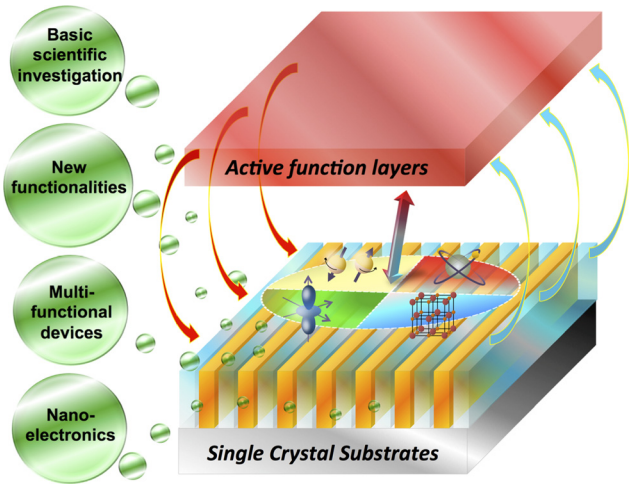


FIG. 11. A general roadmap for developing multifunctionalities with periodic domain patterns as well as the conjunct heterostructures, which paves an innovation way toward to basic scientific investigation, new functionalities, multi-functional devices, and new nanoelectronics.

well-established system hitherto, might provide a general scene to exploit the periodic domain patterns for facilitating the fundamental understanding.

In addition to explore the ferroic domains, the domain walls are sensitive and reacting to the adjacent ferroic orders and thus offer the new playground to discover new functionalities that are absent in the bulk. For example, more recent studies have focused on the coupling between ferromagnets and specific domain walls since the domain walls have created an anomalous environment to accommodate the local spin state, charge distribution, electronic structure, and strain. A recent study found a correlation not to the density of domain walls but to the density of certain types of domain walls that determine the magnetic coupling with other conjunct materials.[107] Further experiment processed by Martin *et al*. has confirmed the role of the domain wall types in determining the exchange bias interaction, which took place between pinned, uncompensated spin occurring at domain walls in BFO, and spins in the ferromagnetic layer. It has been evidenced that the heterostructure made of magnetic layer and randomly distributed 109° domain walls exhibit significantly enhanced exchange bias. An exchange enhancement interaction has arisen from an interaction of the spins in the ferromagnet and the fully compensated (001) surface of the BFO 109° domain walls, resulting in an enhancement of the coercive field of the ferromagnetic layer. The combination of periodic multiferroic patterns with the ferromagnets could be used to reveal the local spin environments, which help researchers to design advanced sensor, or magnetic information storage devices.

Given that the modification of adjacent environment gives rise to the entirely different functionalities at the walls, the next level question is: how to integrate the similar modulation process and multifunctionalities into a real device? The limited tunability and efficiency are still challenging factors with regard to a real device composed of a single ferroic material. As a result, several applications have been proposed to integrate the functional domains in ferroic systems based on their conjugation and effects on existing devices.[108–110] Despite the fact that both experimental discoveries and theoretical investigations prosper in recent years, further realization remains to be explored. Another scenario should be depicted are the challenges to determine whether these fascinating functionalities can be controlled at sufficiently high speeds and long life time to enable new logic devices or nanoelectronics. Factors such as switching speed, domain switching and motion dynamics, and corresponding size effects need to be carefully studied and improved to reach practical applications. More efforts are ongoing for renovating the field of nanoelectronics. Overall, the advanced engineering and multifunctionalities of ferroic domains is a rapid growing subject that will no doubt attract more attention in the near future.

To sum up, we hope this review has covered the main idea for discovering and developing the exciting multifunctionalities within the periodic domain patterns, especially from the perspective of multiferroic materials. The intriguing properties and rich phenomena found and based on ferroic patterns form a growing and exciting field of interest. Through advanced domain engineering, we use periodic domain patterns of multiferroic BFO as a model system to explore how to precisely control the domain architectures and different types of domain walls. The resulting periodic patterns have been used to push both the fundamental studies and advanced applications in the manner either the ferroic systems themselves or heterostructures with functional layers. Having reviewed the promising functionalities and potential advantages of the periodic domains, this review also concerns the future challenges and practical applications. The progresses while building up fundamental understanding and pursuing the practical applications of the multifunctional domain patterns in ferroic systems have suggested the solutions to the major scientific questions human beings have faced nowadays.

## ACKNOWLEDGMENTS

This work was supported by the National Science Council of Republic of China (under contract No. NSC-101-2119-M-009-003-MY2), Ministry of Education (grant No. MOE-ATU 101W961), and the Center for Interdisciplinary Science at National Chiao Tung University.

[1]V. K. Wadhawan, *Introduction to Ferroic Materials* (Gordon & Breach, UK, 2000).
[2]A. L. Roitburd, Phys. Status Solidi A **37**, 329 (1976).
[3]N. Sridhar, J. M. Rickman, and D. J. Srolovitz, Acta Mater. **44**, 4085 (1996).
[4]N. Sridhar, J. M. Rickman, and D. J. Srolovitz, Acta Mater. **44**, 4097 (1996).
[5]N. A. Spaldin, *Magnetic Materials: Fundamentals and Device Applications* (Cambridge, UK, 2003).
[6]W. Eerenstein, N. D. Mathur, and J. F. Scott, Nature **442**, 759 (2006).
[7]R. Ramesh and N. A. Spaldin, Nature Mater. **6**, 21 (2007).
[8]S. W. Cheong and M. Mostovoy, Nature Mater. **6**, 13 (2007).
[9]T. Zhao, A. Scholl, F. Zavaliche, K. Lee, M. Barry, A. Doran, M. P. Cruz, Y. H. Chu, C. Ederer, N. A. Spaldin, R. R. Das, D. M. Kim, S. H. Baek, C. B. Eom, and R. Ramesh, Nature Mater. **5**, 823 (2006).
[10]Y. H. Chu, L. W. Martin, M. B. Holcomb, M. Gajek, S. J. Han, Q. He, N. Balke, C. H. Yang, D. Lee, W. Hu, Q. Zhan, P. L. Yang, A. Fraile-

Rodríguez, A. Scholl, S. X. Wang, and R. Ramesh, Nature Mater. **7**, 478 (2008).
[11]R. R. Das, D. M. Kim, S. H. Baek, C. B. Eom, F. Zavaliche, S. Y. Yang, R. Ramesh, Y. B. Chen, X. Q. Pan, X. Ke, M. S. Rzchowski, and S. K. Streiffer, Appl. Phys. Lett. **88**, 242904 (2006).
[12]P. Fischer, M. Polomska, I. Sosnowska, and M. Szymanski, J. Phys. C: Solid State Phys. **13**, 1931 (1980).
[13]Y. N. Venevtsev, G. Zhadanow, and S. Solov'ev, Sov. Phys. Crystallogr. **4**, 538 (1960).
[14]G. A. Smolenski, V. A. Isupov, A. I. Agranovskaya, and N. N. Krainik, Sov. Phys. Solid State **2**, 2651 (1961).
[15]R. Seshadri and N. A. Hill, Chem. Mater. **13**, 2892 (2001).
[16]F. Kubel and H. Schmid, Acta. Cryst. B **46**, 698 (1990).
[17]F. Zavaliche, S. Y. Yang, T. Zhao, Y.-H. Chu, M. P. Cruz, C. B. Eom, and R. Ramesh, Phase Trans. **79**, 991 (2006).
[18]I. E. Dzyaloshinskii, Sov. Phys. JETP **5**, 1259 (1957).
[19]T. Moriya, Phys. Rev. **120**, 91 (1960).
[20]C. Ederer and N. A. Spaldin, Phys. Rev. B **71**, 060401 (2005).
[21]C. Ederer and N. A. Spaldin, Phys. Rev. B **71**, 224103 (2005).
[22]H. Béa, M. Bibes, S. Cherifi, F. Nolting, B. Warot-Fonrose, S. Fusil, G. Herranz, C. Deranlot, E. Jacquet, K. Bouzehouane, and A. Barthélémy, Appl. Phys. Lett. **89**, 242114 (2006).
[23]S. M. Wu, S. A. Cybart, D. Yi, J. M. Parker, R. Ramesh, and R. C. Dynes, Phys. Rev. Lett. **110**, 067202 (2013).
[24]J. C. Yang, Q. He, S. J. Suresha, C. Y. Kuo, C. Y. Peng, R. Haislmaier, M. A. Motyka, G. Sheng, C. Adamo, H. J. Lin, Z. Hu, L. Chang, L. H. Tjeng, E. Arenholz, N. J. Podraza, M. Bernhagan, R. Uecker, D. G. Schlom, V. Gopalan, L. Q. Chen, C. T. Chen, R. Ramesh, and Y. H. Chu, Phys. Rev. Lett. **109**, 247606 (2012).
[25]A. Lubk, S. Gemming, and N. A. Spaldin, Phys. Rev. B **80**, 104110 (2009).
[26]S. K. Streiffer, C. B. Parker, A. E. Romanov, M. J. Lefevre, L. Zhao, J. S. Speck, W. Pompe, C. M. Foster, and G. R. Bai, J. Appl. Phys. **83**, 2742 (1998).
[27]A. E. Romanov, M. J. Lefevre, J. S. Speck, W. Pompe, S. K. Streiffer, and C. M. Foster, J. Appl. Phys. **83**, 2754 (1998).
[28]J. Fousek and V. Janovec, J. Appl. Phys. **40**, 135 (1969).
[29]W. Ren, Y. Yang, O. Diéguez, J. Íñiguez, N. Choudhury, and L. Bellaiche, Phys. Rev. Lett. **110**, 187601 (2013).
[30]N. A. Pertsev, A. G. Zembilgotov, and A. K. Tagantsev, Phys. Rev. Lett. **80**, 1988 (1998).
[31]Y. L. Li, S. Y. Hu, Z. K. Liu, and L. Q. Chen, Acta Mater. **50**, 395 (2002).
[32]D. D. Fong, A. M. Kolpak, J. A. Eastman, S. K. Streiffer, P. H. Fuoss, G. B. Stephenson, C. Thompson, D. M. Kim, K. J. Choi, C. B. Eom, I. Grinberg, and A. M. Rappe, Phys. Rev. Lett. **96**, 127601 (2006).
[33]I. A. Luk'yanchuk, A. Schilling, J. M. Gregg, G. Catalan, and J. F. Scott, Phys. Rev. B. **79**, 144111 (2009).
[34]Y. H. Chu, Q. He, C. H. Yang, P. Yu, L. W. Martin, P. Shafer, and R. Ramesh, Nano Lett. **9**, 1726 (2009).
[35]Y. C. Chen, C. H. Ko, Y. C. Huang, J. C. Yang, and Y. H. Chu, J. Appl. Phys. **112**, 052017 (2012).
[36]Y. H. Chu, M. P. Cruz, C. H. Yang, L. W. Martin, P. L. Yang, J. X. Zhang, K. Lee, P. Yu, L. Q. Chen, and R. Ramesh, Adv. Mater. **19**, 2662 (2007).
[37]A. N. Morozovska, R. K. Vasudevan, P. Maksymovych, S. V. Kalinin, and E. A. Eliseev, Phys. Rev. B **86**, 085315 (2012).
[38]M. P. Cruz, Y. H. Chu, J. X. Zhang, P. L. Yang, F. Zavaliche, Q. He, P. Shafer, L. Q. Chen, and R. Ramesh, Phys. Rev. Lett. **99**, 217601 (2007).
[39]Y. Wang, C. Nelson, A. Melville, B. Winchester, S. Shang, Z. K. Liu, D. G. Schlom, X. Q. Pan, and L. Q. Chen, Phys. Rev. Lett. **110**, 267601 (2013).
[40]Y. C. Chen, Q. R. Lin, and Y. H. Chu, Appl. Phys. Lett. **94**, 122908 (2009).
[41]L. Landau and E. Lifshitz, Phys. Z. Sowjenunion **8**, 153 (1935).
[42]C. Kittel, Phys. Rev. **70**, 965 (1946).
[43]W. Kinase and H. Takahashi, J. Phys. Soc. Jpn. **12**, 464 (1957).
[44]D. J. Craik and P. V. Cooper, Phys. Lett. A **33**, 411 (1970).
[45]A. A. Thiele, J. Appl. Phys. **41**, 1139 (1970).
[46]M. Hehn, S. Padovani, K. Ounadjela, and J. P. Bucher, Phys. Rev. B **54**, 3428 (1996).
[47]J. L. Bjorkstam and R. E. Oettel, Phys. Rev. **159**, 427 (1967).
[48]A. M. Bratkovsky and A. P. Levanyuk, Phys. Rev. Lett. **84**, 3177 (2000).
[49]W. Pompe, X. Gong, Z. Suo, and J. S. Speck, J. Appl. Phys. **74**, 6012 (1993).
[50]G. Catalan, H. Béa, S. Fusil, M. Bibes, P. Paruch, A. Barthélémy, and J. F. Scott, Phys. Rev. Lett. **100**, 027602 (2008).
[51]R. Takahashi, Ø. Dahl, E. Eberg, J. K. Grepstad, and T. Tybell, J. Appl. Phys. **104**, 064109 (2008).
[52]A. Kopal, T. Bahnik, and J. Fousek, Ferroelectrics **202**, 267 (1997).
[53]C. T. Nelson, B. Winchester, Y. Zhang, S. J. Kim, A. Melville, C. Adamo, C. M. Folkman, S. H. Baek, C. B. Eom, D. G. Schlom, L. Q. Chen, and X. Q. Pan, Nano Lett. **11**, 828 (2011).
[54]J. Seidel, L. W. Martin, Q. He, Q. Zhan, Y. H. Chu, A. Rother, M. E. Hawkridge, P. Maksymovych, P. Yu, M. Gajek, N. Balke, S. V. Kalinin, S. Gemming, F. Wang, G. Catalan, J. F. Scott, N. A. Spaldin, J. Orenstein, and R. Ramesh, Nature Mater. **8**, 229 (2009).
[55]Y. J. Qi, Z. H. Chen, C. W. Huang, L. H. Wang, X. D. Han, J. L.Wang, P. Yang, T. Sritharan, and L. Chen, J. Appl. Phys. **111**, 104117 (2012).
[56]R. G. P. McQuaid, L. J. McGill, P. Sharma, A. Gruverman, and J. M. Gregg, Nat. Commun. **2**, 404 (2011).
[57]Y. H. Hsieh, J. M. Liou, B. C. Huang, C. W. Liang, Q. He, Q. Zhan, Y. P. Chiu, Y. C. Chen, and Y. H. Chu, Adv. Mater. **24**, 4564 (2012).
[58]J. Seidel, P. Maksymovych, A. J. Katan, Y. Batra, Q. He, A. P. Baddorf, S. V. Kalinin, C. H. Yang, J. C. Yang, Y. H. Chu, E. K. H. Salje, H. Wormeester, M. Salmeron, and R. Ramesh, Phys. Rev. Lett. **105**, 197603 (2010).
[59]J. Guyonnet, I. Gaponenko, S. Gariglio, and P. Paruch, Adv. Mater. **23**, 5377 (2011).
[60]Y. Tokunaga, N. Furukawa, H. Sakai, Y. Taguchi, T. H. Arima, and Y. Tokura, Nature Mater. **8**, 558 (2009).
[61]A. Erbil, Y. Kim, and R. A. Gerhardt, Phys. Rev. Lett. **77**, 1628 (1996).
[62]T. Mizokawa and A. Fujimori, Phys. Rev. Lett. **80**, 1320 (1998).
[63]T. Lottermoser and M. Fiebig, Phys. Rev. B **70**, 220407(R) (2004).
[64]J. Přívratská and V. Janovec, Ferroelectrics **204**, 321 (1997).
[65]J. Přívratská and V. Janovec, Ferroelectrics **222**, 23 (1999).
[66]M. Daraktchiev, G. Catalan, and J. F. Scott, Ferroelectrics **375**, 122 (2008).
[67]G. Catalan and J. F. Scott, Adv. Mater. **21**, 2463 (2009).
[68]A. Aird and E. K. H. Salje, J. Phys.: Condens. Matter **10**, L377 (1998).
[69]M. Bartels, V. Hagen, M. Burianek, M. Getzlaff, U. Bismayer, and R. Wiesendanger, J. Phys.: Condens. Matter **15**, 957 (2003).
[70]D. Meier, J. Seidel, A. Cano, K. Delaney, Y. Kumagai, M. Mostovoy, N. A. Spaldin, R. Ramesh, and M. Fiebig, Nature Mater. **11**, 284 (2012).
[71]T. Choi, Y. Horibe, H. T. Yi, Y. J. Choi, Weida Wu, and S.-W. Cheong, Nature Mater. **9**, 253 (2010).
[72]T. Sluka, A. K. Tagantsev, P. Bednyakov, and N. Setter, Nat. Commun. **4**, 1808 (2013).
[73]A. Tselev, V. Meunier, E. Strelcov, W. A. Shelton, I. A. Luk'yanchuk, K. Jones, R. Proksch, A. Kolmakov, and S. V. Kalinin, ACS Nano **4**, 4412 (2010).
[74]D. A. Allwood, G. Xiong, C. C. Faulkner, D. Atkinson, D. Petit, and R. P. Cowburn, Science **309**, 1688 (2005).
[75]L. Thomas, M. Hayashi, X. Jiang, R. Moriya, C. Rettner, and S. S. P. Parkin, Science **315**, 1553 (2007).
[76]S. S. P. Parkin, M. Hayashi, and L. Thomas, Science **320**, 190 (2008).
[77]L. Thomas, R. Moriya, C. Rettner, and S. S. P. Parkin, Science **330**, 1810 (2010).
[78]J. Slonczewski, J. Magn. Magn. Mater. **159**, L1 (1996).
[79]L. Berger, Phys. Rev. B **54**, 9353 (1996).
[80]S. S. P. Parkin, X. Jiang, C. Kaiser, A. Panchula, K. Roche, and M. Samant, Proc. IEEE **91**, 661 (2003).
[81]Q. He, C. H. Yeh, J. C. Yang, G. Singh-Bhalla, C. W. Laing, P. W. Chiu, G. Catalan, L. W. Martin, Y. H. Chu, J. F. Scott, and R. Ramesh, Phys. Rev. Lett. **108**, 067203 (2012).
[82]Y. P. Chiu, Y. T. Chen, B. C. Huang, M. C. Shih, J. C. Yang, Q. He, C. W. Liang, J. Seidel, Y. C. Chen, R. Ramesh, and Y. H. Chu, Adv. Mater. **23**, 1530 (2011).
[83]G. Catalan, J. Seidel, R. Ramesh, and J. F. Scott, Rev. Mod. Phys. **84**, 119 (2012).
[84]H. Béa and P. Paruch, Nature Mater. **8**, 168 (2009).
[85]S. Y. Yang, J. Seidel, S. J. Byrnes, P. Shafer, C. H. Yang, M. D. Rossell, P. Yu, Y. H. Chu, J. F. Scott, J. W. Ager III, L. W. Martin, and R. Ramesh, Nat. Nanotechnol. **5**, 143 (2010).
[86]R. Guo, L. You, L. Chen, D. Wu, and J. L. Wang, Appl. Phys. Lett. **99**, 122902 (2011).
[87]A. Bhatnagar, A. R. Chaudhuri, Y. H. Kim, D. Hesse, and M. Alexe, Nat. Commun. **4**, 2835 (2013).

[88]J. T. Heron, M. Trassin, K. Ashraf, M. Gajek, Q. He, S. Y. Yang, D. E. Nikonov, Y. H. Chu, S. Salahuddin, and R. Ramesh, Phys. Rev. Lett. **107**, 217202 (2011).
[89]P. Yu, Y. H. Chu, and R. Ramesh, Mater. Today **15**, 320 (2012).
[90]L. You, C. Lu, P. Yang, G. Han, T. Wu, U. Luders, W. Prellier, K. Yao, L. Chen, and J. Wang, Adv. Mater. **22**, 4964 (2010).
[91]L. You, B. Wang, X. Zou, Z. S. Lim, Y. Yang, D. Hui, C. Lang, and J. Wang, Phys. Rev. B **88**, 184426 (2013).
[92]S. Sahoo, S. Polisetty, C. G. Duan, S. S. Jaswal, E. Y. Tsymbal, and C. Binek, Phys. Rev. B **76**, 092108 (2007).
[93]S. Geprägs, A. Brandlmaier, M. Opel, R. Gross, and S. T. B. Goennenwein, Appl. Phys. Lett. **96**, 142509 (2010).
[94]P. Borisov, A. Hochstrat, X. Chen, W. Kleemann, and C. Binek, Phys. Rev. Lett. **94**, 117203 (2005).
[95]X. He, Y. Wang, N. Wu, A. N. Caruso, E. Vescovo, K. D. Belashchenko, P. A. Dowben, and C. Binek, Nature Mater. **9**, 579 (2010).
[96]V. Laukhin, V. Skumryev, X. Martí, D. Hrabovsky, F. Sánchez, M. V. García-Cuenca, C. Ferrater, M. Varela, U. Lüders, J. F. Bobo, and J. Fontcuberta, Phys. Rev. Lett. **97**, 227201 (2006).
[97]V. Skumryev, V. Laukhin, I. Fina, X. Martí, F. Sánchez, M. Gospodinov, and J. Fontcuberta, Phys. Rev. Lett. **106**, 057206 (2011).
[98]T. H. E. Lahtinen, J. O. Tuomi, and S. van Dijken, Adv. Mater. **23**, 3187 (2011).
[99]J. Kabelac, S. Ghosh, P. S. Dobal, and R. Katiyar, J. Vac. Sci. Technol., B **25**, 1049 (2007).
[100]V. R. Palkar, J. John, and R. Pinto, Appl. Phys. Lett. **80**, 1628 (2002).
[101]J. F. Ihlefeld, A. Kumar, V. Gopalan, D. G. Schlom, Y. B. Chen, X. Q. Pan, T. Heeg, J. Schubert, X. Ke, P. Schiffer, L. W. Martin, Y. H. Chu, and R. Ramesh, Appl. Phys. Lett. **91**, 071922 (2007).
[102]Y. H. Chu, Q. Zhan, L. W. Martin, M. P. Cruz, P. L. Yang, F. Zavaliche, S. Y. Yang, J. X. Zhang, L. Q. Chen, D. G. Schlom, I. N. Lin, T. B. Wu, and R. Ramesh, Adv. Mater. **18**, 2307 (2006).
[103]Y. H. Chu, L. W. Martin, M. B. Holcomb, and R. Ramesh, "Controlling magnetism with multiferroics," Mater. Today **10**(10), 16-23 (2007).
[104]F. Saurenbach and B. D. Terris, Appl. Phys. Lett. **56**, 1703 (1990).
[105]O. Kolosov, A. Gruverman, J. Hatano, K. Takahashi, and H. Tokumoto, Phys. Rev. Lett. **74**, 4309 (1995).
[106]A. V. Levlev, S. Jesse, A. N. Morozovsk, E. Strelcov, E. A. Eliseev, Y. V. Pershin, A. Kumar, V. Y. Shur, and S. V. Kalinin, Nat. Phys. **10**, 59 (2014).
[107]L. W. Martin, Y. H. Chu, M. B. Holcomb, M. Huijben, P. Yu, S. J. Han, D. Lee, S. X. Wang, and R. Ramesh, Nano Lett. **8**, 2050 (2008).
[108]V. Garcia, S. Fusil, K. Bouzehouane, S. Enouz-Vedrenne, N. D. Mathur, A. Barthelemy, and M. Bibes, Nature (London) **460**, 81 (2009,).
[109]P. Maksymovych, S. Jesse, P. Yu, R. Ramesh, A. P. Baddorf, and S. V. Kalinin, Science **324**, 1421 (2009).
[110]A. Q. Jiang, C. Wang, K. J. Jin, X. B. Liu, J. F. Scott, C. S. Hwang, T. A. Tang, H. B. Lu, and G. Z. Yang, Adv. Mater. **23**, 1277 (2011).